HEAT AND MASS TRANSFER IN THE CONDENSER–EVAPORATOR OF A DYNAMIC SYSTEM FOR WATER EXTRACTION FROM AN ELECTROCHEMICAL ENERGY GENERATOR

L. S. Starodubov, A. R. Gordon,
and M. A. Gordon

UDC 532.546:536.242:621.352.6

A system of transfer equations over the length of the apparatus is considered, taking account of the electrolyte-concentration gradient in a porous phase separator. The results of computer calculation are given.

Analytical description of heat- and mass-transfer processes over the length of an apparatus is difficult because of the unwieldiness of the solutions obtained. In calculating the condenser–evaporator of a dynamic system for water extraction from an electrochemical generator (ECG), there are additional difficulties associated with the need to take account of the difference in alkali concentration in the porous separator of the liquid and gas phases; extension of the evaporation zone into the depth of the porous separator complicates the problem even more. In [1], the influence of the separative porous membrane with possible increase in depth of the phase boundary was taken into account by experimental means.

Consider conditions of porous-membrane operation in which there is no increase in depth.

Evaporation of electrolyte from a porous material is accompanied by filtrational flow of electrolyte in capillaries under the action of capillary forces. The velocity of this flow is equal in magnitude to the velocity of Stefan flow in a liquid. Bending of the meniscus in capillaries of the evaporator membrane is due both to the pressure difference existing on both sides of the membrane between the vapor–hydrogen mixture and the electrolyte flux (the pressure of the vapor–gas mixture exceeds the electrolyte pressure) and to the hydraulic pressure difference in the capillary due to filtrational flow of electrolyte. Thus, the capillary pressure in evaporation is

$$P_C = P_m - P_e + \Delta P_f. \tag{1}$$

With increase in intensity of evaporation, the meniscus sags; there is no movement into the depth of the porous material until P_C exceeds a critical value equal to the pressure determined by the height of maximum liquid lift in the capillary.

If, for example, a porous metal–ceramic phase separator of thickness 0.1 mm with a mean pore diameter of the order of 1 μm is used in a condenser–evaporator for the extraction of water with flux densities of the order of 1 $g/cm^2 \cdot h$, the capillary pressure determined from Eq. (1) will not reach the limiting value for this phase separator, which is 2 kg/cm^2, that is, no increase in depth will be observed.

In heat and mass transfer, vapor–gas mixtures separate into quasihomogeneous and inhomogeneous. In an inhomogeneous vapor–gas mixture, the molecular masses and thermophysical properties of the components forming the mixture are markedly different, and heat and mass transfer has its distinctive features [2, 3].

Heat and mass transfer in the condenser–evaporator of a dynamic system for water extraction from an electrochemical generator, which is a transfer process in an inhomogeneous vapor–gas mixture, is expediently described on the basis of the results of [4]. In [4], the change in intensity of heat and mass transfer, taking account of the transverse flux of material (the numbers Nu and Nu_D), with respect to their intensity in the absence or slight presence of a transverse flux (to the numbers Nu_1 and Nu_{D1}) is written in the form of a dependence on the absolute value of $\varepsilon_{2\infty}/\Pi g$ and the mixture-inhomogeneity factor $\bar{M}$. Taking into account that $Nu_1 \cong Nu_{D1}$, the dependence in [4] is such that, with decrease in density of the transverse mass flux, i.e., with increase in the parameter $|\varepsilon_{2\infty}/\Pi g|$, the processes of heat and mass transfer occur in the region of complete analogy both for evaporation and for condensation. In

---

Translated from Inzhenerno-Fizicheskii Zhurnal, Vol. 49, No. 4, pp. 640-648, October, 1985.

0022-0841/85/4904-1213$09.50

the region of large $|\varepsilon_{2\infty}/\Pi g|$ equality of the thermal Nusselt number and the diffusional Nusselt number determined by the intensity of the diffusional component of the transverse mass flux is first observed, i.e., $\mathrm{Nu} = \mathrm{Nu}_D\varepsilon_{20}$, and then, at large gas contents at the wall, total analogy of the processes of heat and mass transfer is seen ($\mathrm{Nu} = \mathrm{Nu}_D$); the influence of the inhomogeneity factor $\bar{M}$ is weakened with decrease in the transverse flux density.

Calculation of the evaporator–condenser is now undertaken for the region $|\varepsilon_{2\infty}/\Pi g| \geqq 10$, where

$$\frac{\mathrm{Nu}_D\varepsilon_{20}}{\mathrm{Nu}_{D1}} \simeq 1. \tag{2}$$

The deviation of the left-hand side of Eq. (2) from unity in real conditions may be obtained by comparison with the results of [4], taking into account that $\varepsilon_2 = \Pi g(\varepsilon_{2\infty}/\Pi g - 1)$. Thus, when $\bar{M} = 1$ and $|\varepsilon_{2\infty}/\Pi g| = 10$, the deviation is -6% for evaporation and $+6\%$ for condensation. The influence of the inhomogeneity factor $\bar{M}$ introduces additional errors in Eq. (2). For a mixture of hydrogen with water vapor, $\bar{M} = 9$, which leads to -3% additional error in evaporation when $|\varepsilon_{2\infty}/\Pi g| = 10$ and leads to almost no additional error for condensation. In analyzing the error of Eq. (2), it must be taken into account that a misprint appears in [4], unfortunately; see Eq. (23) of [5], for example. In [4], Eq. (20) should appear in the form

$$\mathrm{Nu}_D\,\Pi g/\mathrm{Nu}_{D1} = (\varepsilon_{2\infty}/\Pi g - 0{,}4)^{-1}\Phi(\bar{M}).$$

Consider the calculation of heat and mass transfer in an evaporator–condenser for the example of an evaporation chamber with a direct-flow scheme of heat-carrier motion. The thermal load and productivity of the chamber with respect to water will be determined as a function of the input parameters of the electrolyte and vapor–gas mixture.

Taking account of Eq. (2), the mass-transfer coefficient is determined by the expression

$$\beta_p = \frac{D_p \mathrm{Nu}_{D1} P_\mathrm{m}}{d(P_\mathrm{m} - P_{10})}, \tag{3}$$

where

$$D_p = \frac{D_\mathrm{cI}}{R_1 T}\left(\frac{T}{273}\right)^{1,8}\frac{P_\mathrm{I}}{P_\mathrm{m}}.$$

The equations describing the heat and mass transfer from the electrolyte to the vapor–gas mixture may be written in the form

$$\alpha_\mathrm{e}(t_\mathrm{e} - t_0) = -\frac{dI_\mathrm{e}}{dF}; \tag{4}$$

$$\alpha_\mathrm{e}(t_\mathrm{e} - t_0) = \frac{dI_\mathrm{m}}{dF}; \tag{5}$$

$$\alpha_\mathrm{e}(t_\mathrm{e} - t_0) = \alpha_\mathrm{m}(t_0 - t_\mathrm{m}) + jr; \tag{6}$$

$$P_{10} = f(t_0, c_0); \tag{7}$$

$$j = \frac{D\gamma}{\mu\delta}\ln\frac{c_0}{c_\mathrm{e}}; \tag{8}$$

$$j = \beta_P(P_{10} - P_{1\infty}). \tag{9}$$

In Eqs. (4)-(9), the enthalpy of the electrolyte is $G_\mathrm{e}C_{p\mathrm{e}}t_\mathrm{e}$ and the enthalpy of the vapor–gas mixture not including mist is [6]

$$I_\mathrm{m} = [C_{P2}t + (597.4 + 0{,}43t)X]G_2;$$

$$X = \frac{G_1}{G_2} = \frac{9P_{1\infty}}{P_\mathrm{m} - P_{1\infty}}.$$

The heat of phase transition is determined from the formula proposed in [6]

$$r = 597{,}4 - 0{,}57t_0.$$

The vapor pressure of water above the solution of potassium hydroxide P_{10} (kg/m^2) in the temperature range 60-100°C and the alkali concentration range 24-45 mass % is written in the form

$$P_{10} = (842 - 4.5\cdot 10^{-3}t_0^2 q_0 + 0{,}291t_0^2 + 0.425t_0 q_0 - 28.425t_0 - 12{,}5q_0)\,13{,}596.$$

The flux density of water diffusing in the porous structure of the phase separator – Eq. (8) – is described by the relation from [7].

For convenience of calculation, taking into account that $\rho \cong \gamma[1 + (q/100)]$ and $c = \rho q/100$, it may be established that

$$j \simeq \frac{\gamma D}{\mu\delta} \ln\left[\frac{(100 + q_0)\,q_0}{(100 + q_e)\,q_e}\right].$$

The diffusion coefficient of water in a solution of potassium hydroxide D (m^2/h) is written in the form

$$D = 20.16\cdot 10^{-3} \exp\left(-\frac{2246}{273 + t_0}\right).$$

In Eq. (9), the vapor pressure in the flux is conveniently expressed in terms of the vapor flow rate from the relation for the moisture content of hydrogen

$$P_{1\infty} = P_m \cdot \frac{G_1}{9G_2 + G_1}.$$

Consider the change in alkali concentration in the electrolyte flux over the length of the apparatus.

The quantity q_e may be defined as

$$q_e = \frac{G_{al}}{G_e}\cdot 100\,\%. \tag{10}$$

From Eq. (10),

$$\frac{dq_e}{dF} = -\frac{G_{al}}{G_e^2}\cdot 100\,\%\,\frac{dG_e}{dF}. \tag{11}$$

Substituting $g_{al} = G_e q_e/100\%$ into Eq. (11) gives

$$\frac{dq_e}{dF} = -\frac{q_e}{G_e}\,\frac{dG_e}{dF}. \tag{12}$$

In describing the mass transfer, it must be taken into account that $dG_1/dF = -dG_e/dF = jE$.

Differential equations for calculating the heat and mass transfer in an evaporator with a direct-flow system of motion of the electrolyte and vapor–gas mixture are presented below. The equations are obtained under the assumption of constant Nu_{D1}, α_e, α_m over the length of the apparatus and are written without taking account of the thermal drag of the evaporator wall

$$\frac{dG_1}{dF} = \frac{D_{\mathbf{cI}}(t_m + 273)^{0,8}\mathrm{Nu}_{D1}P_I}{R_1 273^{1,8} d\,(P_m - P_{10})}\left(P_{10} - P_m\,\frac{G_1}{9G_2 + G_1}\right); \tag{13}$$

$$\frac{dG_e}{dF} = -\frac{\gamma 20.16\cdot 10^{-3}\exp\left(-\dfrac{2246}{273 + t_0}\right)}{\mu\delta}\ln\left[\frac{(100 + q_0)\,q_0}{(100 + q_e)\,q_e}\right]; \tag{14}$$

$$\frac{dt_m}{dF} = \frac{\alpha_e(t_e - t_0) - (597.4 + 0.43t_m)\,j}{3.4G_2 + 0.43G_1}; \tag{15}$$

$$\frac{dt_e}{dF} = -\frac{\alpha_e(t_e - t_0) + C_{pe}t_e\dfrac{dG_e}{dF}}{C_{pe}G_e}; \tag{16}$$

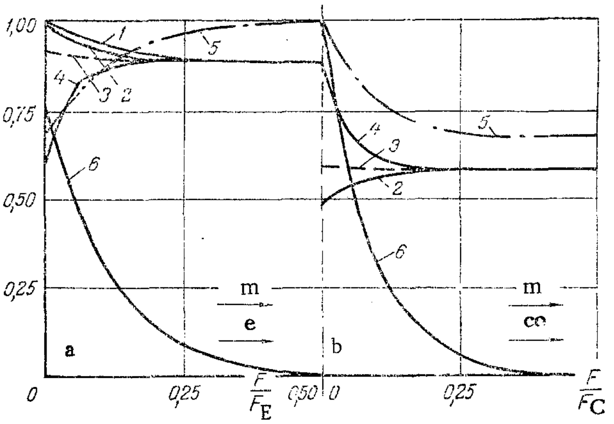

Fig. 1. Evaporator–condenser. Direct flow: a) evaporator; b) condenser. The arrows indicate the direction of heat-carrier motion ($G^{in}_{e} = G^{in}_{co} = 10$ kg/h; $G^{in}_{1E} = G^{in}_{1C} = 0.158$ kg/h; $G_2 = 0.25$ kg·h; $t^{in}_{e} = 80°C$; $t^{in}_{co} = 40°C$; $t^{in}_{m.E} = t^{in}_{m.C} = 46.6°C$; $F_E = F_C = 0.064$ m^2; $P_m = 1.6 \cdot 10^4$ kg/m^2; $Nu_{D1} = 7.5$; $\alpha_m = 300$ kcal/m^2·h·deg; $\alpha_e = \alpha_{co} = 2000$ kcal/m^2·h·deg; $d = 4 \cdot 10^{-3}$ m; $\mu = 5$; $\delta = 1 \cdot 10^{-4}$ m; $C_{pe} = 0.7$ kcal/kg·deg; $q^{in}_{e} = 35$ mass %); 1) alkali concentration at the evaporation surface; 2) temperature of electrolyte (in condenser of coolant) 3) wall temperature; 4) temperature of vapor–hydrogen mixture; 5) flow rate of water vapor; 6) density of transverse vapor flux.

$$\frac{dq_e}{dF} = -\frac{q_e}{G_e}\frac{dG_e}{dF}. \tag{17}$$

The system in Eqs. (13)-(17) is solved for the following initial conditions: $G_1 = G^{in}_{1}$; $G_e = G^{in}_{e}$, $t_m = t^{in}_{m}$, $t_e = t^{in}_{e}$, $q_e = q^{in}_{e}$ when $F = 0$. That the parameters at the wall P_{10}, t_0, q_0 and the density of the transverse vapor flux are initially unknown complicates the solution; however, these parameters may be determined from the algebraic system in Eqs. (6)-(9).

The solution of Eqs. (13)-(17) has been obtained on a computer by the Euler method. In each step of the iteration, the parameters P_{10}, t_0, q_0, and j are determined from Eqs. (6)-(9) by Newton's method.

The integration is taken over the course of the vapor–gas mixture with a variable step; the whole of the surface F_E, equal to $6.4 \cdot 10^{-2}$ m^2, is divided into three sections of $0.2F_E$, $0.3F_E$, and $0.5F_E$, respectively. For the first section, the integration step is $2 \cdot 10^{-4}$ m^2; for the second, $4 \cdot 10^{-4}$ m^2; for the third, $8 \cdot 10^{-4}$ m^2. The solution obtained is shown in Fig. 1a.

Note that the analytical temperature dependence of the saturated vapor pressure above pure water was given in [6], for example.

Consider the operation of the evaporator–condenser as a whole [1].

Dry hydrogen arrives at the evaporator–condenser, and then passes successively through alternating evaporation and condensation chambers, thus removing the water forming in the ECG electrolyte.

The electrolyte and the coolant are separated from the vapor–gas mixture by a porous separator of gas and liquid phases; the electrolyte chambers are connected in parallel, and the coolant chambers are also connected together. Steady heat and mass transfer in the chambers is established after a few chambers in the course of hydrogen motion.

In Fig. 1 this steady process in the evaporation and condensation chambers is shown in dimensionless form with a direct-flow scheme of heat-carrier motion. For Fig. 1 the thermal load of the evaporation chamber is equal to the thermal load of the condensation chamber, and is 69.6 kcal/h; the productivity with respect to the condensate is equal to the amount of moisture evaporated and is 76.2 g/h; the maximum transverse vapor flux density (in the

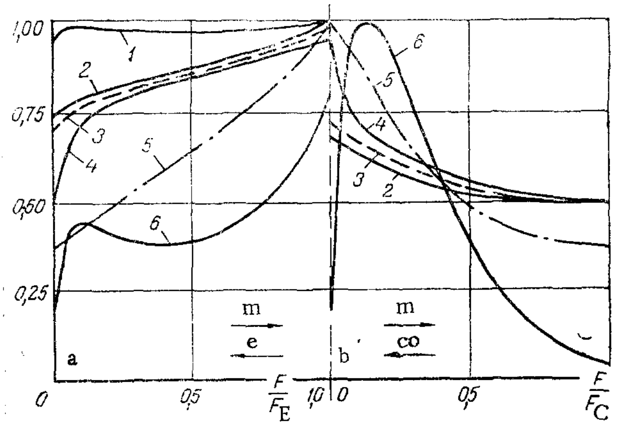

Fig. 2. Evaporator–condenser. Counterflow: a) evaporator; b) condenser. The arrows indicate the direction of heat-carrier motion ($G^{in}_e = G^{in}_{co} = 10$ kg/h; $G^{in}_{1E} = G^{in}_{1C} = 0.112$ kg/h; $G_2 = 0.25$ kg/h; $t^{in}_e = 80°C$; $t^{in}_{co} = 40°C$; $t^{in}_{m.E} = t^{in}_{m.C} = 40.03°C$; $F_E = F_C = 0.064$ m^2; $P_m = 1.6 \cdot 10^4$ kg/m^2; $Nu_{D1} = 7.5$; $\alpha_m = 300$ kcal/m^2·h·deg; $\alpha_e = \alpha_{co} = 2000$ kcal/m^2·h·deg; $d = 4 \cdot 10^{-3}$ m; $\mu = 5$; $\delta = 1 \cdot 10^{-4}$ m; $C_{pe} = 0.7$ kcal/kg·deg; $q^{in}_e = 35$ mass %): 1) alkali concentration at the evaporation surface; 2) electrolyte temperature (in condenser, coolant temperature); 3) wall temperature; 4) temperature of vapor–hydrogen mixture; 5) water–vapor flow rate; 6) transverse vapor flux density.

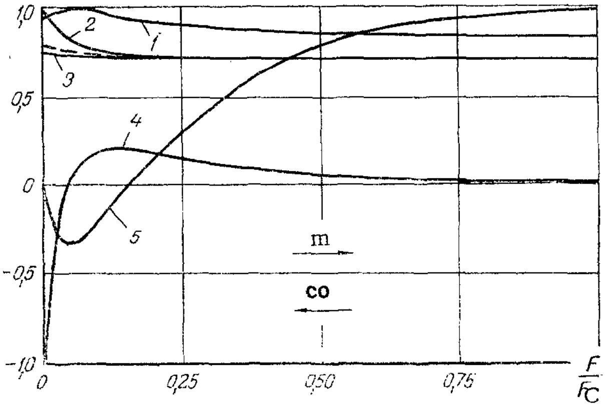

Fig. 3. Condenser. Counterflow. The arrows indicate the direction of heat-carrier motion; the wall temperature is shown as a dashed curve ($G^{in}_{co} = 5$ kg/h; $G^{in}_1 = 0.094$ kg/h; $G_2 = 0.160$ kg/h; $t^{in}_{co} = 42.7°C$; $t^{in}_m = 60.2°C$; $F = 0.064$ m^2; $P_m = 1.6 \cdot 10^4$ kg/m^2; $Nu_{D1} = 7.5$; $\alpha_m = 300$ kcal/m^2·h·deg; $\alpha_{co} = 2000$ kcal/m^2·h·deg; $d = 4 \cdot 10^{-3}$ m): 1) water–vapor flow rate; 2) temperature of vapor–hydrogen mixture; 3) coolant temperature; 4) transverse vapor flux density; 5) productivity of apparatus with respect to water.

condenser) is 13 kg/m^2·h; the alkali concentration at the evaporation surface on entering the evaporator is 39.8 mass %.

Usually, the productivity of an ECG evaporator–condenser with respect to condensate is small in comparison with the coolant and electrolyte flow rates through the apparatus; therefore, the change in coolant and electrolyte flow rate over the length of the apparatus may be neglected, as may the change in concentration in the electrolyte flux over the length of the apparatus.

This may be used to simplify the analysis of heat and mass transfer in a condenser–evaporator with a counterflow scheme of heat-carrier motion.

The solution of the problem for counterflow may be performed analogously to the direct-flow case, if the temperature of the electrolyte and coolant at the output from the apparatus is specified in some approximation. In that case, beginning the differentiation with the temperatures adopted at the output, it is necessary to approach the specified temperature of coolant and electrolyte at the input to the apparatus; if the temperatures specified and obtained at the input do not agree, then the output temperatures must be adjusted. A search algorithm for the real temperatures at the output is simpler to write in that the input and output temperatures are directly related.

The steady process of heat and mass transfer in evaporation and condensation chambers with a counterflow scheme of heat-carrier motion is shown in Fig. 2. The input parameters and coefficients for the operating conditions in Fig. 2 are taken to be the same as for the conditions in Fig. 1, except for the water-vapor flow rate and the temperature of the vapor–gas mixture at the evaporator input, which take different values in the ECG in view of the change in direction of motion of the heat carrier. The thermal load of both the evaporator and condenser chambers for Fig. 2 is 148 kcal/h; the productivity with respect to condensate and the amount of moisture evaporated are 0.184 kg/h; the maximum transverse vapor flux density is observed in calculations in the condenser and is 6.3 $kg/m^2 \cdot h$; the alkali concentration at the evaporation surface at the output with respect to the electrolyte is 37.5 mass %.

It is of interest to compare the operation of direct-flow and counterflow schemes of heat-carrier motion. As is evident from Fig. 1, in direct flow, heat and mass transfer occur practically over only a quarter of the surface, whereas in counterflow the evaporation and condensation surfaces are more completely involved. The thermal-load ratio of direct flow and counterflow is 0.47; the ratio of the corresponding productivities with respect to condensate is 0.41. It also follows from Figs. 1a and 2 that, in direct flow, the maximum transverse vapor flux density is observed at the input to the condenser, whereas in counterflow it is observed at approximately 0.12 of its length in the direction of motion of the vapor–hydrogen mixture.

A particular case of evaporator–condenser operation in an ECG is shown in Figs. 1 and 2, for chosen input parameters and parameters of the apparatus itself. Of course, the change in these parameters influences the distribution of heat-carrier parameters over the length of the apparatus. For example, with one set of parameters at the input, "humps" in the transverse vapor flux density may not be observed at all; with another set, change in wall temperature may lead to change even in the direction of the transverse vapor flux in the condenser and evaporator, in direct flow and counterflow.

Consider the operating conditions of an evaporator in a direct-flow scheme of heat-carrier motion with the following parameters: $t^{in}{}_e = 50°C$; $t^{in}{}_m = 90°C$; $G^{in}{}_1 = 0.3$ kg/h; $G_2 = 0.5$ kg/h; $G^{in}{}_e =$ kg/h; $q^{in}{}_e = 35$ wt. %; $P_m = 1.6 \cdot 10^4$ kg/m^2; $Nu_{D1} = 7.5$; $\alpha_m = 300$ $kcal/m^2 \cdot h \cdot deg$; $\alpha_e = 2000$ $kcal/m^2 \cdot h \cdot deg$; $F = 0.064$ m^2, $\mu = 5$; $d = 4 \cdot 10^{-3}$ m; $\delta = 1 \cdot 10^{-4}$ m; $C_{pe} = 0.7$ kcal/kg·deg. Such an evaporator will condense 4 g/h vapor in its initial section; in its subsequent sections it will operate as an evaporator, working at a rate of 20 g/h of moisture.

For the given example, the vapor pressure of water above the surface of the potassium hydroxide is $P_{10} = (162.2 - 2.42 \cdot 10^{-3} t_0^2 q_0 + 0.138 t_0 q_0 + 0.137 t_0^2 - 7.73 t_0 - 2.96 q_0) \cdot 13.596$.

An example of condenser operation in counterflow, in which the transverse flow changes direction, is shown in Fig. 3.

As follows from Fig. 3, evaporation occurs in the initial section, constituting 0.05 of the surface (curve 4); then the transverse flux changes direction. The transverse vapor flux density at the input to the apparatus with respect to the vapor–gas mixture is 3.3 $kg/m^2 \cdot h$. The amount of moisture evaporated in the apparatus is 3.8 g/h. In a section equal to 0.15 of the surface, the productivity of the apparatus with respect to water is zero, since the amount of water condensed in this section is equal to the amount which evaporates. Increase in vapor content in the vapor–hydrogen mixture at the beginning of the process, with subsequent decrease, is reflected by the trend of curve 1. The amount of condensate from the point at which the productivity of the apparatus with respect to water is zero to the output from the apparatus with respect to the vapor–gas mixture is 11.4 g/h. The difference in coolant enthalpy at the output and input is 17.2 kcal/h.

Graphical results of the calculation give a clear idea of the change in parameters over the length of the apparatus, allow the magnitude of the evaporator–condenser working surface of ECG to be more correctly estimated, and show that, in some conditions, change in direction of the transverse vapor flux may occur, both in condensers and in evaporators.

The machine time required (UVK M-4030) for two variants of counterflow conditions in an evaporator is 2 min.

NOTATION

P, pressure; $\varepsilon_{2\infty} = P_{2\infty}/P_m$, volume content of gas in the basic mass of vapor–gas mixture; $\varepsilon_{20} = P_{20}/P_m$, volume content of gas at the wall; $\Pi g = (P_{10} - P_{1\infty})/P_m$, dimensionless difference in partial pressures; $\bar{M} = M_1/M_2$, nonuniformity factor of mixture; M, molecular mass; Nu_{D1}, mass-transfer Nusselt number with a vanishingly small influence of the transverse mass flux; D_p, diffusion coefficient of water vapor in hydrogen, referred to the partial-pressure gradient; D_c, mutual diffusion coefficient; R, individual gas constant; d, equivalent channel diameter of vapor–gas mixture; γ, density of pure water; I, enthalpy; μ, attenuation coefficient of diffusion of porous structure; δ, thickness of porous phase separator; α, heat-transfer coefficient; C_p, specific heat; X, moisture content of hydrogen; c, alkali concentration, g/cm^3; q, alkali concentration, mass %; ρ, density of solution; j, transverse vapor flux density; F, surface of apparatus. Indices: 1, water vapor; 2, hydrogen; m, vapor–gas mixture; 0, at evaporation or condensation surface; ∞, in flow; E, evaporator; C, condenser; e, electrolyte; co, coolant; in, input parameter; out, output parameter; al, dry alkali.

LITERATURE CITED

1. V. K. Shchitnikov and V. S. Bogachev, "Evaporation–condensation system of water removal from the electrolyte of the fuel elements in an electrochemical generator," in: Heat and Mass Transfer in Electrochemical Energy Generators [in Russian], A. V. Lykov Institute of Heat and Mass Transfer, Academy of Sciences, BSSR, Minsk (1981), pp. 79-98.
2. L. D. Berman, "Influence of inhomogeneity of the vapor–gas mixture on the mass transfer in evaporation and sublimation," Teor. Osn. Khim. Tekhnol., No. 6, 811-819 (1976).
3. L. D. Berman, "Influence of the inhomogeneity of the vapor–gas mixture on the mass transfer in condensation," Teor. Osn. Khim. Tekhnol., No. 6, 911-915 (1977).
4. L. D. Berman, "Generalization of experimental data on heat and mass transfer in evaporation and condensation," Teploenergetika, No. 4, 8-13 (1980).
5. L. D. Berman, "Heat and mass transfer in a vapor–gas phase with intense evaporation of liquids," in: Heat Transfer and Hydrodynamics. Proceedings of the Fifth All-Union Conference on Heat Transfer and Hydraulic Drag in the Motion of a Two-Phase Flux in Elements of Power Machinery and Equipment [in Russian], Nauka, Leningrad Branch, Leningrad (1977).
6. A. V. Nesterenko, Principles of Thermodynamic Calculations of Ventilation and Air Conditioning [in Russian], Vysshaya Shkola, Moscow (1965).
7. A. R. Gordon, L. S. Starodubov, and V. R. Zayavlin, "Stefan flow in liquids," Inzh.-Fiz. Zh., 34, No. 6, 1059-1065 (1978).